A Time-Resolved 4-tap Image Sensor Using Tapped PN-Junction Diode Demodulation Pixels

Hiroaki Nagae[1], Shohei Daikoku[1], Keita Kondo[1], Keita Yasutomi[1,2],

Keiichiro Kagawa[1,2], Shoji Kawahito[1,2]

[1]Graduate School of Integrated Science and Technology, Shizuoka University,

Hamamatsu, 432-8011, Japan

[2]Research Institute of Electronics, Shizuoka University, Hamamatsu, 432-8011, Japan

E-mail: hnaga@idl.rie.shizuoka.ac.jp

I. Introduction

Time-resolved lock-in pixel image sensors using multiple-tap demodulation pixels are expected to be used for a variety of applications such as indirect TOF imagers and biological fields. Numerous demodulation pixel structures have been reported to date [1][2][3][4][5]. In order to enhance the time resolution of lock-in pixel imagers, high-speed demodulation pixel structures with a large photo-detection area for high-sensitivity and small parasitic sensitivity are desired. As one of candidates to meet the requirements, we have presented a demodulation pixel with a tapped pn-junction diode (TPD) structure at IISW 2019[5]. In the previous report, the device concept of the 4-tap TPD demodulator and its characterizations of DC photo response only are presented. In this paper, a newly-implemented 4-tap TPD pixel with improved modulation characteristics by using a fixed-potential electrode in the center and the results of their characterizations is presented.

II. Pixel Design and simulation

Fig.1 shows the top and cross-sectional view of the proposed pixel which is based on the 4-tap TPD demodulator structure reported in [5]. The newly-designed 4-tap demodulator with a center-tap p+ electrode (TC) applied a fixed potential has a more-effective electric-field modulation in the photo-detection area for fast photo-carrier response, low parasitic light sensitivity (PLS) and the resulting high demodulation contrast to short light-pulse operation. Fig.2 shows a simulated 1-D potential plot along X1-X1' and X2-X2', and the 2-D potential plot at the depth(z) of 1um when -0.5V, -1.5V and -2V are applied to the T3, TC and other terminals (T1, T2 and T4), respectively. As shown in this figure, a uniform large electric field (0.15V/um) is created for the width of 6um and a large potential modulation ratio ($\Delta V_C/\Delta V_T$=0.9V/1.5V=60%) is attained while forming a sufficient potential barrier between the adjacent p+ taps for preventing hole leakage current.

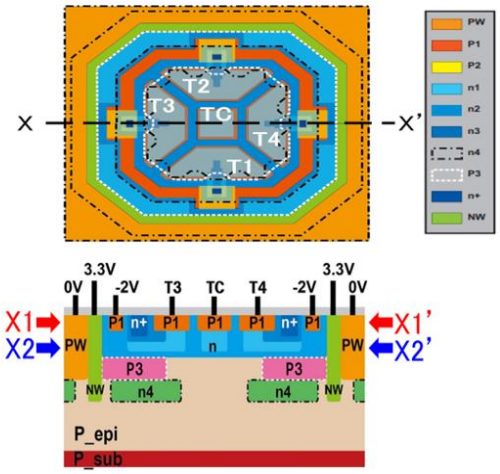

Fig.1 4-tap TPD demodulator.

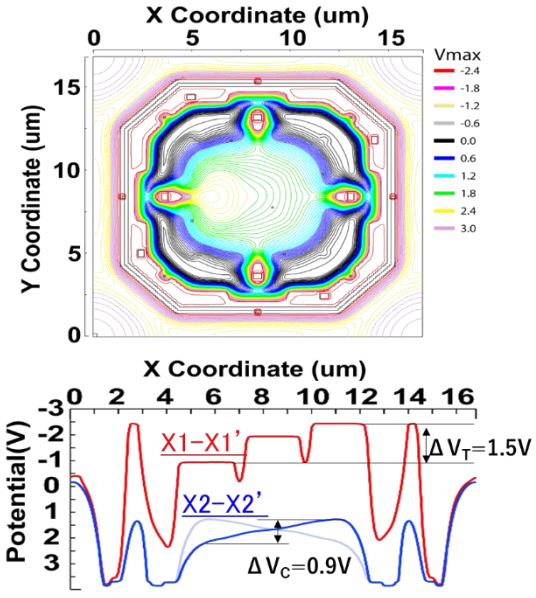

Fig.2: 1-D and 2-D plots of simulated potential of 4-tap TPD demodulator (T1:0[V], TC:-1.5[V], T2,T3,T4:-2[V]).

III. Measured results

Measured results of the implemented pixels are shown in Fig. 3 and Table I. These modulation curves are obtained by driving the p+ electrode according to the timing chart on the left, and delaying the light pulse. The biasing conditions are as follows: HIGH and LOW voltage levels for T1, T2, T3 and T4 are -0.5V and -2V, respectively, and the voltage levels of TC and the back bias are -1.5V and -2V, respectively. The laser with the wavelength of 850nm, pulse width of 8ns and the cycle time of 200ns is used. The number of light pulses applied is 50,000 cycles. As shown in Table 1, a high demodulation contrast, or a high charge modulation ratio (=(peak output of each tap)/(the sum of all the outputs)) of over 90% is attained.

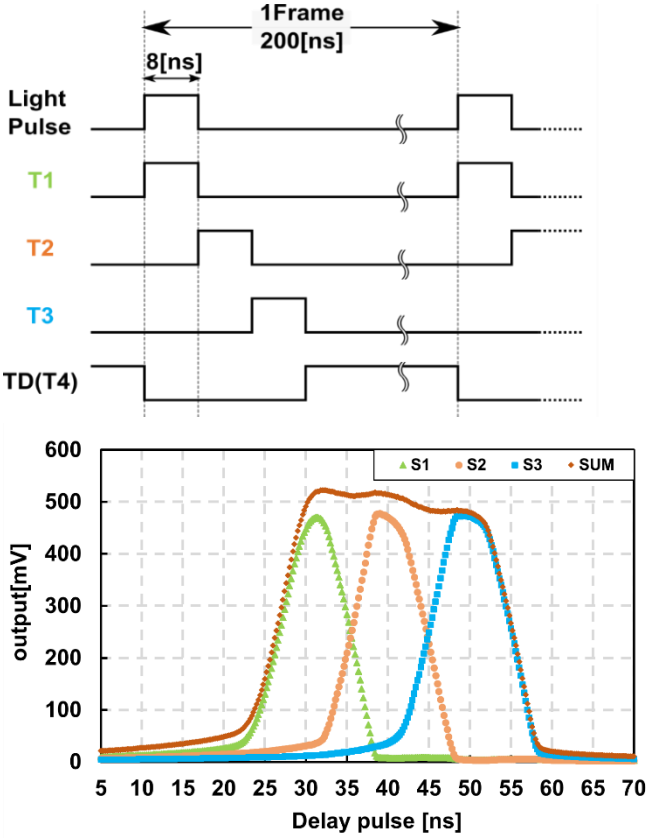

Fig.3: Timing chart and modulation characteristics.

Table. I: Charge modulation ratio.

	Peak of output [mV]	Sum of all outputs [mV]	Charge modulation ratio [%]
S1	470.2	519.1	90.6
S2	477.6	517.1	92.4
S3	473.3	482.2	98.2

In order to characterize the pixel response quantitatively, the impulse response of the sensor was measured under the same conditions but with a short-pulse light source (pulse width: 69 ps, wavelength: 851 nm). The results are shown in Fig. 4(a) and its natural logarithm of the time derivative is shown in Fig. 4(b). To obtain the sensor response from this result, we must consider an impulse response model. The output response of the sensor is obtained by convolution of the gate response, the sensor response, and the light pulse response. In this case, since short pulse laser is used, the output response is mostly dependent on the gate response $g(t)$ given by Eq. (2), and sensor response $f(t)$ given by Eq. (1). From the results of the authors laboratory, the sensor response is supposed to be expressed as an exponential curve given by the form of e^(-t/τ), where τ is the time constant. The horizontal axis of the impulse response is the delay, thus the sensor response is convolved in the opposite direction. K_1 is the time it takes for the slowest electron to move. The rising edge of the impulse response $h(t)$ is expressed as the convolution of $f(t)$ and $g(t)$ given by Eq. (3) and its derivative is given by Eq. (4)

$$f(t) = \begin{cases} e^{\frac{t}{\tau_1}} & (t \le K_1) \\ 0 & (t > K_1) \end{cases} \quad \dots (1)$$

$$g(t) = 1 - e^{-\frac{t}{\tau_2}} \quad \dots (2)$$

$$h(t) = af(t) * g(t) = \begin{cases} a\left(\frac{\tau_1^2}{\tau_1+\tau_2} e^{\frac{t}{\tau_1}} + \frac{\tau_1\tau_2}{\tau_1+\tau_2} e^{-\frac{t}{\tau_2}} - \tau_1\right) & (t \le K_1) \\ a\left\{\frac{\tau_1\tau_2}{\tau_1+\tau_2}\left(1 - e^{\frac{K_1}{\tau_1}} e^{\frac{K_1}{\tau_2}}\right) e^{-\frac{t}{\tau_2}} + \tau_1\left(e^{\frac{K_1}{\tau_1}} + 1\right)\right\} & (t > K_1) \end{cases} \quad \dots (3)$$

$$\frac{dh(t)}{dt} = \begin{cases} a\left\{\frac{\tau_1}{\tau_1+\tau_2}\left(e^{\frac{t}{\tau_1}} - e^{-\frac{t}{\tau_2}}\right)\right\} & (t \le K_1) \\ a\left\{\frac{\tau_1}{\tau_1+\tau_2}\left(e^{\frac{K_1}{\tau_1}} e^{\frac{K_1}{\tau_2}} - 1\right) e^{-\frac{t}{\tau_2}}\right\} & (t > K_1) \end{cases} \quad \dots (4)$$

From Eq. (4), if $\tau_2 < \tau_1 < K_1$, the slope of the natural logarithm of the time derivative around t=K_1 is $1/\tau_1$ (K_1<t) and $-1/\tau_2$ (K_1>t). However, the equation shows that the slope changes abruptly from $1/\tau_1$ to $-1/\tau_2$ at t=K_1, which is different to the Fig. 4(b). Therefore, in the region where t is small, we assume a linear region for the gate response (assuming a slewing of the gate voltage and the rate of change of the potential under the gate). Then g(t) is modified as Eq. (5), where K_2 is the length of the linear region and a constant c is applied to smoothly connect the

linear and exponential region.

$$g(t) = \begin{cases} bt & (t \le K_2) \\ 1 - ce^{-\frac{t}{\tau_2}} & (t > K_2) \end{cases} \quad \dots (5)$$

Then the convolution and its derivative are also modified as Eqs. (6) and (7), where A_1(>0) A_2(<0) and A_3(<0) are constant to avoid complications in the equations.

$$h(t) = af(t) * g(t)$$

$$= \begin{cases} a\,b\tau_1\left(\tau_1 e^{\frac{t}{\tau_1}} - t - \tau_1\right) & (t \le K_2) \\ a\left\{A_1 e^{\frac{t}{\tau_1}} + \dfrac{c\tau_1\tau_2}{\tau_1+\tau_2} e^{-\frac{t}{\tau_2}} - \tau_1\right\} & (K_2 < t \le K_1) \\ a\left\{A_2 e^{\frac{t}{\tau_1}} + \dfrac{c\tau_1\tau_2}{\tau_1+\tau_2} e^{-\frac{t}{\tau_2}} - \tau_1 \right. \\ \quad \left. +\tau_1 b e^{-\frac{K_1}{\tau_1}}(\tau_1 - K_1 + t)\right\} & (K_1 < t \le K_1 + K_2) \\ a\left\{\dfrac{c\tau_1\tau_2}{\tau_1+\tau_2}\left(1 - e^{\frac{K_1}{\tau_1}} e^{\frac{K_1}{\tau_2}}\right) e^{-\frac{t}{\tau_2}}\right. \\ \quad \left. +\tau_1\left(e^{\frac{K_1}{\tau_1}} + 1\right) + A_3\right. & (t > K_1 + K_2) \end{cases} \quad \dots (6)$$

$$\frac{dh(t)}{dt}$$

$$= \begin{cases} ab\tau_1\left(e^{\frac{t}{\tau_1}} - 1\right) & (t \le K_2) \\ a\left\{\dfrac{A_1}{\tau_1} e^{\frac{t}{\tau_1}} - \dfrac{c\tau_1}{\tau_1+\tau_2} e^{-\frac{t}{\tau_2}}\right\} & \\ \approx a\dfrac{A_1}{\tau_1} e^{\frac{t}{\tau_1}}\Big|_{t=K_1} & (K_2 < t \le K_1) \\ a\left\{\dfrac{A_2}{\tau_1} e^{\frac{t}{\tau_1}} - \dfrac{c\tau_1}{\tau_1+\tau_2} e^{-\frac{t}{\tau_2}} + \tau_1 b e^{-\frac{K_1}{\tau_1}}\right\} & (K_1 < t \le K_1 + K_2) \\ a\left\{\dfrac{-c\tau_1}{\tau_1+\tau_2}\left(1 - e^{\frac{K_1}{\tau_1}} e^{\frac{K_1}{\tau_2}}\right) e^{-\frac{t}{\tau_2}}\right. & (K_1 + K_2 < t) \end{cases} \quad \dots (7)$$

From (7), in the region K_1<t<K_2 (especially around t=K_1), the time derivative of output characteristic is determined by the sensor response, and the time constant of the sensor response can be obtained by taking its natural logarithm. In the region K_1 <t< $K_1 + K_2$, the time derivative is expressed as the sum of a constant and an exponential function. In the actual case, the constant of the third term is larger than the other terms, resulting in a characteristic with an almost constant gradient. In the region of K_1+K_2<t, the output response is determined by the gate response, and its natural logarithm is equal to the time constant of the gate response. This result is similar to Fig. 4(b). Applying the appropriate values to each of the constants in (6) and fitting the result to the rise in Fig. 4, the fitting result is as shown in Fig. 5. Although the actual measured values do not match perfectly due to the inclusion of noise, it can be confirmed that the fitted graph and the actual measured values have a close approximation. Based on the above, the response time constant of the sensor can be obtained from the first half of the rise. The time constant of the sensor response obtained from each rising response is shown in Table II. Table II shows that the time constant of the sensor is smaller than 1ns. Therefore, in intrinsic response, this sensor can transfer about 2/3 of the electrons in 1ns and most of the electrons are in 2ns.

Ⅳ. Conclusions.

This paper presents a time-resolved lock-in pixel image sensor based on a tapped PN junction diode structure. The characteristics of multi-tap output, high-speed modulation, and large aperture make this structure suitable for implementing lock-in pixels in longer range TOF image sensors. In this paper, we report the test results of the modulation operation. Various other characteristics are left for a future work.

Acknowledgments

This work was in-part supported by JSPS KAKENHI Grant Number 18H05240 and JST COI-STREAM program.

References

[1] S. Kim et al., “A Three-Dimensional Time-Of-Flight CMOS Image Sensor with Pinned-Photodiode Pixel Structure “, IEEE J. Electron Device Letters, vol. 31, no. 11, pp. 1272-1274, Nov. 2010.

[2] D. Stoppa et al.,” A Range Image Sensor Based on 10-µm Lock-in Pixels in 0.18µm CMOS Imaging Technology ", IEEE J. Solid-State Circuits, vol. 46 no. 1 pp.248-258, Jan.2011.

[3] Y. Kato et al., “320x240 Back-illuminated 10 µm CAPD Pixels for High Speed Modulation Time-Of-Flight CMOS Image Sensor “, IEEE Symp. VLSI Circuits, pp. C288-C289, 2017.

[4] S. Han et al., "A Time-Of-Flight Range Image Sensor with Background Canceling Lock-in Pixels Based on Lateral Electric Field Charge Modulation" IEEE J. Electron Devices Society, vol. 3, no. 3, pp. 267-275, 2015.

[5] S. Kawahito et al., "A Time-Resolved Lock-in Pixel Image Sensor Using Multiple-Tapped Diode and Hybrid Cascade Charge Transfer Structures", Proc. Int. Image Sensor Workshop（IISW）, pp.238-241,2019

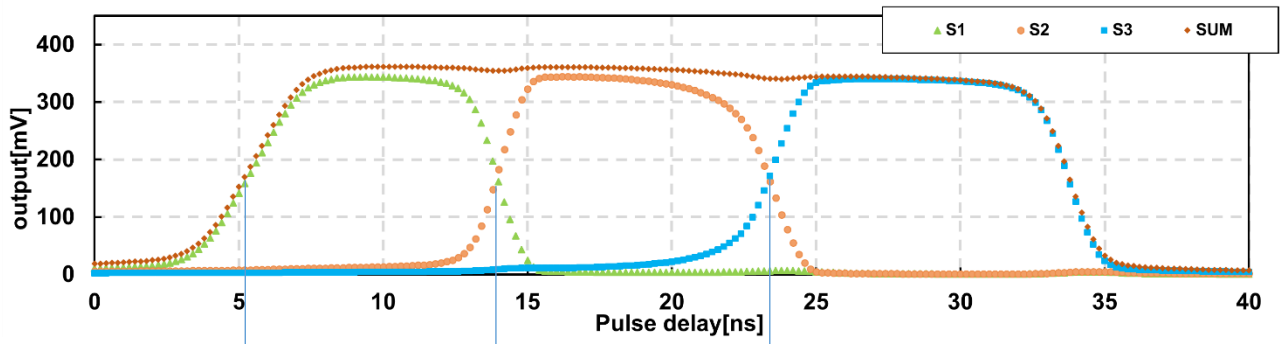

(a) Short-pulse response

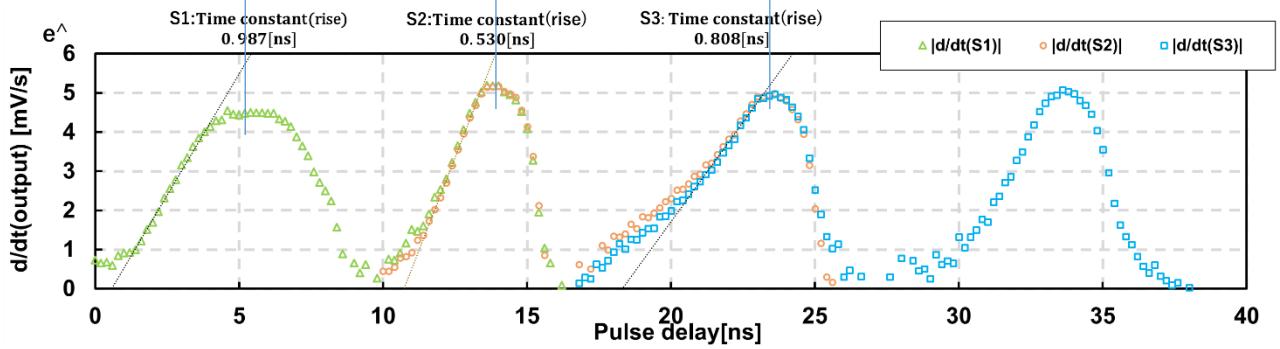

(b) Time derivative of the short-pulse response

Fig.4: Response to a short-pulse

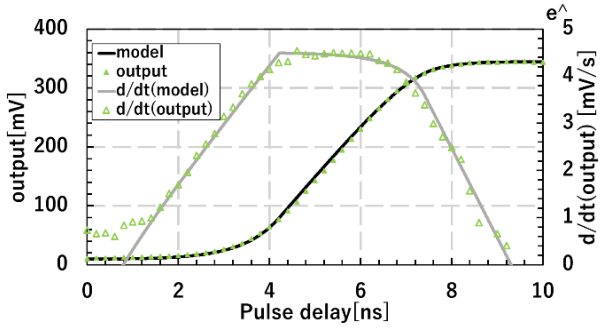

(a)Fitting S1

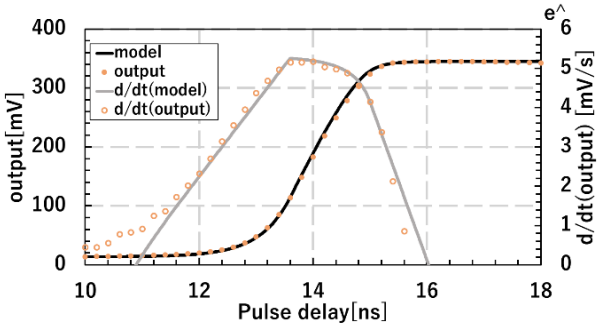

(b)Fitting S2

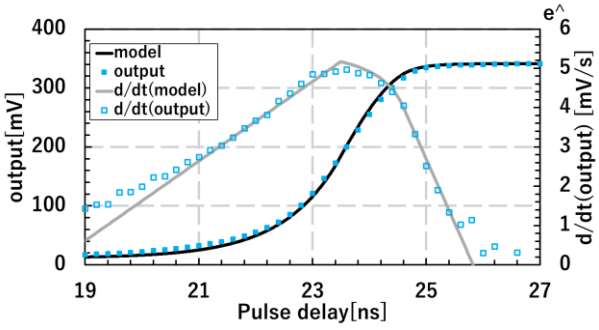

(c)Fitting S3

Fig.5: Fitting output

Table II: Time constant of the response (Intrinsic response)

	Time constant [ps]
S1	987
S2	530
S3	808